

# Illuminating Hot Jupiters in caustic crossing

Sedighe Sajadian and Sohrab Rahvar <sup>\*</sup>

*Department of Physics, Sharif University of Technology,  
P.O.Box 11365–9161, Tehran, Iran*

3 September 2021

## ABSTRACT

In recent years a large number of Hot Jupiters orbiting in a very close orbit around the parent stars have been explored with the transit and doppler effect methods. Here in this work we study the gravitational microlensing effect of a binary lens on a parent star with a Hot Jupiter revolving around it. Caustic crossing of the planet makes enhancements on the light curve of the parent star in which the signature of the planet can be detected by high precision photometric observations. We use the inverse ray shooting method with tree code algorithm to generate the combined light curve of the parent star and the planet. In order to investigate the probability of observing the planet signal, we do a Monte-Carlo simulation and obtain the observational optical depth of  $\tau \sim 10^{-8}$ . We show that about ten years observations of Galactic Bulge with a network of telescopes will enable us detecting about ten Hot Jupiter with this method. Finally we show that the observation of the microlensing event in infra-red band will increase the probability for detection of the exo-planets.

## 1 INTRODUCTION

Gravitational microlensing as one of the applications of general relativity is proposed by Paczyński (1986) for detecting the dark compact halo objects so-called MACHOs in the Galactic halo. While not enough MACHOs have been detected in the halo (Milsztajn & Lasserre 2001), however the microlensing technic has been used as an astrophysical tool for studying the atmosphere of the stars and exploring the exo-planets. In the standard method for exploring planets with the microlensing, a star with the companion planets can play the role of lens and produce caustic lines where crossing the caustics by the source star produces a high magnification on the light curve (Mao & Paczynski 1991). In this case in addition to the standard microlensing light curve we can detect a short duration spark due to the caustic crossing, formed by the planet. A precise photometry of the event is essential to find out this short duration signature of the planet. The advantage of this technic compare to the other methods of the exo-planet detection is that it is sensitive to the observation of earth mass planets (Beaulieu et al. 2006) and also those planets located beyond the snow line (Gould et al. 2010). There is also other methods in gravitational microlensing such as planetary microlensing signals from the orbital motion of the source star around the common barycenter of source star–planet system (Rahvar & Dominik 2009).

In addition to the mentioned methods, Graff & Gaudi (2000) proposed caustic crossing of a close-in Jupiter size planet, produced by a binary lens. In this case the planet’s light is magnified so much that it can be detected by a 10-m class telescope. Here we extend this work looking to the details of the light curves and study the most favorite pass band for this observation. Since in a close-in Jupiter, the thermal emission due to the high temperature of the planet is more significant than the reflected light from the parent star, the observations in the Infra-red pass band is more favorable than the visual pass band. We also do a Monte-Carlo simulation with a given observational strategy to obtain the number of observ-

able events in terms of the parameters of the planet and the parent star. We emphasize that while the observations of the hot Jupiters is simpler in nearby stars via the eclipsing and doppler methods, the microlensing method can detect distant systems and enable us to compare the statistics of the hot Jupiters with the nearby observations. One of the interesting features of the light curve for the planet caustic crossing is that the planet can cross the caustic more than that of parent star, as it traces effectively a longer path due to the revolving motion around the parent star.

The paper is organized as follows. In Section 2 we will introduce the caustic crossing of the parent star and planet system and generate light curve with inverse ray shooting technic, introducing a new development in tree-code algorithm. In section 3 we study the characteristics of the light curve in terms of the orbital parameters of the planet and the parent star. In section 4 we explain our Monte-Carlo simulation for estimating the probability of illuminating Hot Jupiters with this method. In section 5 we give the conclusions.

## 2 MICROLENSING LIGHT CURVE

A binary system deflects the light ray with more complicated way than a single lens. Let us represents  $\xi$  as the position of the image in the lens plane and  $\eta$  the position of the source in the source plane, the geometrical relation between these parameters is given by the lens equation as follows (Schneider & Wiess 1986):

$$\underline{\eta} = \frac{D_s}{D_l} \underline{\xi} - D_{ls} \underline{\alpha}(\underline{\xi}), \quad (1)$$

where underline represents the vector,  $\underline{\alpha}$  is the overall deflection angle due to a double lens and  $D_s$ ,  $D_l$  and  $D_{ls}$  are the distance of the source and lens from the observer and distance between the lens and source, respectively. The deflection angle for the light ray

is given as follows

$$\underline{\alpha}(\underline{\xi}) = \frac{4GM_1}{c^2} \frac{\underline{\xi} - \underline{\rho}_1}{|\underline{\xi} - \underline{\rho}_1|^2} + \frac{4GM_2}{c^2} \frac{\underline{\xi} - \underline{\rho}_2}{|\underline{\xi} - \underline{\rho}_2|^2}, \quad (2)$$

where  $\underline{\rho}_1$  and  $\underline{\rho}_2$  are the positions of the binary system in the lens plane and  $M_1$  and  $M_2$  are mass of the lenses. Equation (1) as the lens equation is a fifth order equation and in general the solution is not trivial. One of the possible solution for solving the lens equation is the inverse ray shooting method (Kayser et al. 1986; Schneider & Wiess 1987). In this method we follow the position of the light ray that shoots from the observer to the lens plane, knowing the position of the lenses we can calculate the deflection angle and substituting in the lens equation results in the position of the source. We pixelize the source and the lens plane and for each light ray passing from the lens plane and hitting the source plane, we count the number of hits inside each pixel. These numbers identify the magnification pattern in the source plane. We use tree code method as we describe it later, for generating the image and the magnification of the source star.

In order to simplify our calculation we take the dimensionless parameters in the lens equation. Let us define the overall Einstein radius as follows:

$$R_E = \sqrt{\frac{4G(M_1 + M_2)}{c^2} \frac{D_l D_{ls}}{D_s}}. \quad (3)$$

We normalize the lens equation to this length scale, which results in:

$$\underline{x} = \underline{r} - \underline{\alpha}(\underline{r}), \quad (4)$$

where  $\underline{x} = D_l/D_s \times \underline{\eta}/R_E$ ,  $\underline{r} = \underline{\xi}/R_E$  and the deflection angle is given by:

$$\underline{\alpha}(\underline{r}) = \mu_1 \frac{\underline{r} - \underline{r}_1}{|\underline{r} - \underline{r}_1|^2} + \mu_2 \frac{\underline{r} - \underline{r}_2}{|\underline{r} - \underline{r}_2|^2} \quad (5)$$

and  $\mu_i = M_i/(M_1 + M_2)$ ,  $\underline{r}_i = \underline{\rho}_i/R_E$ .

We take a straight line for the path of the center of mass of the parent star and planet at the lens plane. Taking the mass of parent star larger than the mass of planet, the parent star follows approximately a straight line as follows:

$$\underline{u}_s = (-u_0 \sin \alpha + \frac{t - t_0}{t_E} \cos \alpha) \hat{i} + (u_0 \cos \alpha + \frac{t - t_0}{t_E} \sin \alpha) \hat{j}, \quad (6)$$

where  $u_0$  is defined as the minimum impact parameter of source star from the center of the cartesian coordinate system, normalized to the Einstein radius,  $t_0$  is time of impact parameter, and  $\alpha$  is angle between  $x$ -axis and the trajectory of the source star. The rotation of the planet around the parent star makes a cycloid like pattern on the source plane which is given by:

$$\begin{aligned} \underline{u}_p &= \underline{u}_s + \tilde{a} [\cos(\omega t + \varphi) \cos(\alpha + \beta) \\ &\quad - \cos(\delta) \sin(\omega t + \varphi) \sin(\alpha + \beta)] \hat{i} \\ &\quad + \tilde{a} [\cos(\omega t + \varphi) \sin(\alpha + \beta) \\ &\quad + \cos(\delta) \sin(\omega t + \varphi) \cos(\alpha + \beta)] \hat{j}, \end{aligned} \quad (7)$$

where  $\tilde{a}$  is the projection of the planet orbit on the lens plane normalized to the Einstein radius,  $\omega$  is the angular velocity of planet around the source star which can be obtained from the Kepler's third law:

$$\omega = \sqrt{\frac{G(M_p + M_*)}{a^3}}, \quad (8)$$

and  $a$  is the orbital radius of the planet,  $\delta$  is the deviation of the

normal vector to the orbital plane of the planet from our line of sight. For the Hot Jupiters due to the tidal interaction of the planet and the parent star we set the eccentricity to zero and one angle is sufficient for describing the orbital plane deviation,  $\beta$  is angle between the trajectory of the source star and the projected semi-major axis of the planet and  $\varphi$  is initial phase of the planet.

In order to generate the light curve, we need the relative velocity of the binary lens with the parent star and companion planet. The relative transverse velocity of the source-observer line of sight with respect to the lens at the lens plane is given by (Kayser et al. 1986):

$$\underline{v}_{rel} = x \underline{v}_s - \underline{v}_l - \underline{v}_o(1 - x), \quad (9)$$

where  $\underline{v}_l$ ,  $\underline{v}_s$  and  $\underline{v}_o$  are the two dimensional transverse velocities of the center of mass of the lens system, source and observer with respect to the line of sight respectively and  $x = D_l/D_s$  is the ratio of the distance of the lens to the source. The velocity of the observer is obtained from the local measurements of the solar system in the Galactic frame. The velocity of the stars in the Bulge is given by the dispersion velocity in this structure and the velocity of the stars in the disk is obtained from the combination of the dispersion and global velocities of the stars (Binney & Tremaine 1987).

Since the lens is a binary system, that will rotate around the center of mass during the microlensing of the parent star and the companion planet. For simplify in our calculation we fix the position of the binary system and obtain the relative motion of the source objects with respect to the rotating binary system. The situation is similar to the studying of the motion of an object in rotating non-intertidal reference frame in the classical mechanics. In the reference frame of the binary system we do the following coordinate transformation for the position of the source object

$$\mathcal{R}(\Omega, \psi) = \begin{pmatrix} \cos \Omega t & -\sin \Omega t \\ \sin \Omega t & \cos \Omega t \end{pmatrix} \quad (10)$$

where  $\Omega$  is the angular velocity of the binary lens, which is given by

$$\Omega = \sqrt{\frac{G(M_1 + M_2)}{d_{\perp}^3}} \cos \psi^3, \quad (11)$$

and  $d_{\perp}$  is the apparent separation of the two lenses from each other and  $\psi$  is the deviation of the normal vector to the binary plane from the line of sight.

For generating the light curve we should note that there are two source objects, the parent star and the planet. The total flux receiving by the observer then is the accumulation of the magnified flux of each component (Han & Gould 1996; Griest & Hu 1992):

$$A_{total} = \frac{F_* A_* + F_p A_p}{F_* + F_p}, \quad (12)$$

where the  $F_*$  and  $F_p$  are the intrinsic flux of the parent star and the planet and  $A_*$  and  $A_p$  are the corresponding magnifications. Let us define the ratio of the intrinsic flux of the planet to the flux of the parent star by  $\varepsilon = F_p/F_*$  which is much smaller than one (i.e.  $\varepsilon \ll 1$ ). The total magnification can be written as:

$$A_{total} = A_* + \varepsilon A_p. \quad (13)$$

For a typical case of the binary lens and a main sequence parent star with an Hot Jupiter companion, the trajectory of the source in the source plane with the corresponding caustic lines is shown in Figure (1). One of the interesting features in the caustic crossing is that while the parent star crosses the caustic lines for two times, the planet due to the cyclic motion approach to the caustic lines more than that of the parent star. The corresponding light curve of the source and planet is shown in Figure (2). Even during the caustic

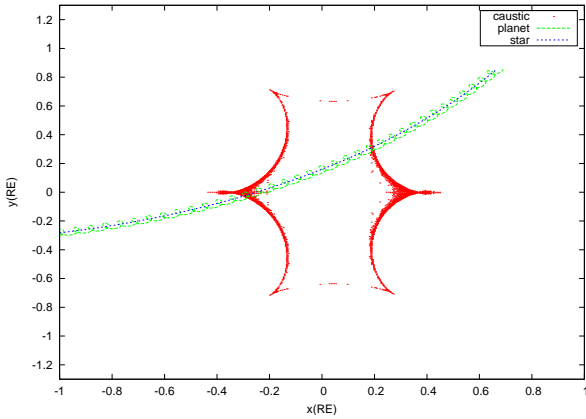


**Figure 1.** The trajectory of the parent star with the companion planet in the source plane is compared with the caustic lines of a binary lens. The scale in this figure is given in terms of overall Einstein radius of a binary lens.

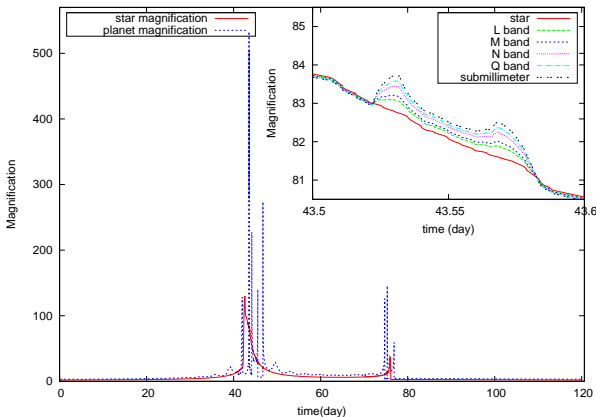


**Figure 2.** The magnification of parent star (solid-line) and the companion planet (dashed-line) in terms of time for the configuration given in Figure (1), for various pass bands. In the top-right hand side of figure, the overall magnification is given in terms of time around the first star's peak surrounded by the two peak of the planet.

crossing of the parent star in the first peak, the planet crosses twice the caustic lines. In order to distinguish the caustic crossing of the planet in the first peak, we zoom in around the first peak of the parent star which is given in the right corner of the Figure (2). We note that the re-crossing of the caustic by the planet takes place with an interval time of about one hour and in order to detect this signal we need a sampling rate less than this time scale.

In the rest of this section we introduce the details in generation of the light curve in the numerical calculation. We should note that the tree code method used in our calculation is different than that introduced by Barnes & Hut (1986) and Wambsganss (1999). In their method the lenses in the lens plane are treated corresponding to their distances to the light ray. In that approach the process of making cells on the lens plane depends on the distance of the lenses to the light ray and their distribution. For the weak gravitational regime where the deflection angle is obtained from the superposition of each lenses, the closer lenses enter to the calculation of the deflection angle with more accuracy than the distant ones. This method can be used for a large number of lenses as the passage of a Quasar light ray through a galaxy.

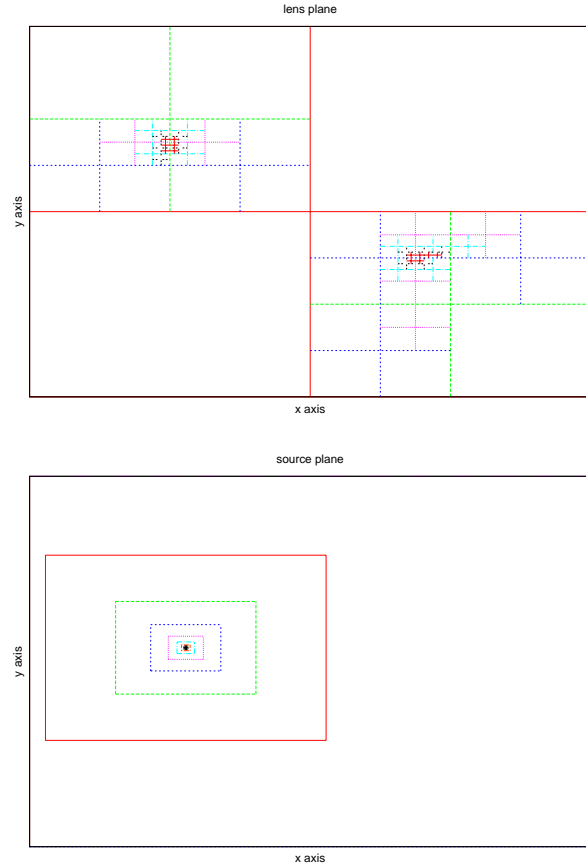


**Figure 3.** Pixelizing process is depicted in this figure. The Upper panel represents the lens plane and the lower panel is the source plane. We take the same size pixel for these two planes during the dividing process. For generating the light curves as shown in Fig. (2), we cover the parent star with  $5 \times 5$  grille.

In our tree code method we divide the lens plane into the cells and choose a same size pixel to surround the source at the source plane. The procedure starts with dividing the lens plane into four parts and in the source plane we choosing a pixel with the same size to surround the source object where the source is located at the center of the cell. We shoot enough number of light rays to each cell in the lens plane to cover the cell's area. Using the lens equation, if at least one of the rays collides to the source cell, we accept that cell for the next dividing step otherwise we remove this cell from the lens plane. We continue this dividing procedure up to the stage that we have enough pixels to cover the source object, having reasonable resolution. As much as smaller cells provides better resolution and less statistical fluctuations in the magnification calculation. Since this pixelizing is time consumer, specially in the Monte-Carlo simulation, we stop the dividing procedure up to a desire resolution. For instance for the parent star, we cover the source with a  $5 \times 5$  grille. Figure (3) depicts the pixelizing procedure in this algorithm. In the final stage of pixelizing, the remained number of cells in the lens plane to that of cells in the source plane that covers the source star provides the magnification due to the gravitational lensing. Also the remained pixels in the lens plane provides the shape of the images. We should note that due to the smaller size of the planet with respect to the source star, the magnification of the planet dose not suffer as much as the parent star from the finite-size effect. The result of planet caustic crossing will be like a flashing,

let's call it "planet flashing". While this flashing in term of magnification is much larger than that of magnification of the source star (see Figure 2), the intrinsic flux of the planet relative to the flux of the source star should be sufficient to be observed by a telescope. In the next section we will discuss this issue in details.

### 3 CHARACTERISTICS OF THE LIGHT CURVE

In this section we study the details of light curve looking to the physical specifications of the source star and the companion planet as well as the binary lens. One of the main factors in the observability of the planet by this method is the ratio of the planet's flux as the signal to the flux of parent star as the background. Using equation (13) we can describe the signal to the background in terms of the total and parent star magnifications:

$$\frac{\delta F}{F} = \frac{A_{total}}{A_*} - 1. \quad (14)$$

The overall flux receiving from a planet to the observer contains the radiation of the thermal energy due to the intrinsic temperature of the planet and the reflection of the parent star's light. Assuming the thermal emission of the planet as a black body radiation (Lopez-Morales & Seager 2007), the temperature of the planet can be calculated by taking into account the absorption of the radiation receiving from the parent star and reradiating it through the Boltzmann law. Hence the planet's temperature is given by:

$$T_p = T_* \left( \frac{R_*}{a} \right)^{1/2} [f(1 - A_B)]^{1/4}, \quad (15)$$

where  $R_*$  and  $T_*$  are the radius and the temperature of the parent star,  $A_B$  is the Bond albedo and  $f$  describes the fraction of reradiating energy which is absorbed by the planet. Recent studies on the difference between the day and night luminosity of the planets through eclipsing show that  $f$  can change between  $1/4$  and  $2/3$  (Harrington et al. 2006; Knutson et al. 2007).  $f = 2/3$  represents a Hot Jupiter with low advection where in this case there is a big different between the temperature of the day and night on the planet and  $f = 1/4$  represents a planet with high redistribution of energy.

The thermal flux of the planet is given by the Planck's law as

$$I(\nu, T_p) = \frac{2h\nu^3}{c^2} (e^{\frac{h\nu}{kT_p}} - 1)^{-1}, \quad (16)$$

where  $I(\nu, T_p)$  represents the emitted power per unit area of emitting surface, per unit solid angle and per unit frequency. Integrating over the frequency and over an half-sphere results in the Stefan-Boltzmann law as follows:

$$F_p^{(th)} = \left( \frac{R_p}{D_s} \right)^2 \sigma T_p^4, \quad (17)$$

where  $R_p$  is the radius of the planet. On the other hand the flux of the planet due to the reflection of parent star's light is given by

$$F_p^{(ref)} = F_* A_g \left( \frac{R_p}{a} \right)^2 g(\Phi), \quad (18)$$

where  $A_g$  is the geometrical albedo, assuming the Lambert's law,  $A_g = 2/3 A_B$ ,  $\Phi$  is the phase of the planet and  $g(\Phi)$  is a function of the planet phase indicates a fraction of the lighted area of planet in front of the observer. Now the ratio of overall planet's flux which is composed by the thermal and reflection terms to the star's flux is given by:

$$\frac{F_p}{F_*} = g(\Phi) \left[ A_g \left( \frac{R_p}{a} \right)^2 + \left( \frac{R_p}{R_*} \right)^2 \left( \frac{T_p}{T_*} \right)^4 \right], \quad (19)$$

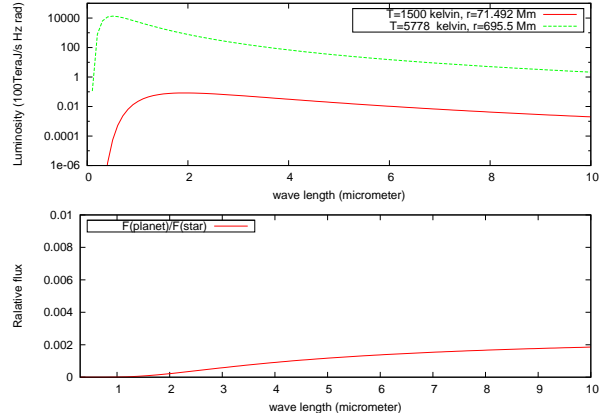


**Figure 4.** Comparison of luminosity between the parent star and the planet. At the upper panel, solid line represents the luminosity of the planet with  $T_p = 1500 K$  and the dashed line is given for the parent star with  $T_* = 5778 K$ . The radius of the planet and the source star is given in Megameter. The lower panel shows the ratio of the luminosity for the planet to the parent star.

where eliminating the planet's temperature from equation (15), the flux ratio obtains in the simpler form of

$$\frac{F_p}{F_*} = \left( \frac{R_p}{a} \right)^2 [A_g + f(1 - A_B)] g(\Phi). \quad (20)$$

The important point in this equation is that it is independent of the temperature and the radius of the source star and it depends only on the chemical composition of the planet atmosphere which changes  $A_B$ , the size and the distance of the planet from the parent star. During the gravitational lensing we multiply the corresponding magnifications of the planet and the parent star to the intrinsic flux of the source objects and obtain the overall receiving flux.

In practice we do not integrate over all the wavelengths, as the detector of the telescope may sensitive to an specific pass band. To find the optimal wavelength for the detection, we maximize the ratio of the intensity of the planet to that of the the parent star, i.e.  $\delta I(\nu)/I(\nu)$ . Using equation (16) and (18), assuming a constant reflection index for all the wavelengths (i.e.  $dA_g/d\nu \simeq const$ ), this ratio obtain as:

$$\frac{\delta I(\nu)}{I(\nu)} = \left[ \left( \frac{R_p}{a} \right)^2 \frac{dA_g}{d\nu} + \frac{e^{\frac{h\nu}{kT_*}} - 1}{e^{\frac{h\nu}{kT_p}} - 1} \left( \frac{R_p}{R_*} \right)^2 \right] g(\Phi). \quad (21)$$

We should note that the reflection flux is mainly important in the optical bands, where the thermal flux dominates in the infra-red and sub-millimeter wavelengths.

Hot Jupiters have small albedo of  $A_g \leq 0.2$  (Rowe et al. 2008), so most of the radiation of the parent star is absorbed by the planet's atmosphere and is reradiated in the infra-red band. The result is a small share of luminosity of the planet in the reflected flux. The exception in the Hot Jupiters happens in the cases with the period of motion smaller than three days. This class of Hot Jupiters so-called Very Hot Jupiters has a surface temperature larger than  $2500 K$  in which they reradiate considerable amount of thermal flux in the optical pass band. However, the peak of the spectrum is in infra-red band (Lopez-Morales & Seager 2007). Out of this exception, the most Hot Jupiters have a considerable flux in infra-red due to the thermal emission (Deming & Seager 2009). We plot equation (21) in Figure (4) as an evidence that in the infra-red pass band, we have the most contrast between the flux of the planet and the

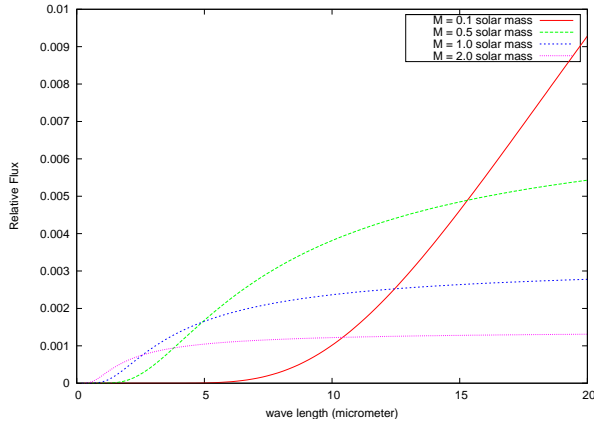


**Figure 5.** The ratio of the planet flux to the parent star as a function of wavelength for four different mass of the parent star. The size and the distance of the planet is fixed to the Jupiter mass with an orbital radius of  $0.05 A.u.$

parent star. Here we compare the planet luminosity to the parent star luminosity as a function of the wavelength. In order to see the sensitivity of this fraction to the mass of the parent star, we plot this function for four masses of the parent star. Choosing the parent star as a main sequence star, the radius of the star can be eliminated in favor of the mass, using

$$R_{\star} = M_{\star}^{0.8}, \quad (22)$$

where the corresponding parameters are normalized to that of sun's values. Figure (5) shows that M-dwarf stars are more favorable for the Hot Jupiter detection in the wavelengths longer than  $15 \mu m$ . However, we should note that for the M-dwarf star, the abundance of the Hot Neptunes is more than the Hot Jupiters (Ida & Lin 2005).

#### 4 MONTE-CARLO SIMULATION

In this section we do a Monte-Carlo simulation to obtain quantitatively the sensitivity of the planet detection to the parameters of the binary lens and the planetary system. Finally we provide the probability for detecting desired events.

First of all we need to generate the parameters of the lens and the source according to the physical distribution of the parameters. We divide the parameter space into the lens and the source parameters for better analyzing. For the lens parameters we take  $q = M_1/M_2$ , the ratio of the masses in the binary system to change uniformly in the range of  $q \in [0, 1]$ , the mass of one of the lenses is taken from the Salpeter mass function (Salpeter 1995) in the range of  $M_1 \in [0.1, 3] M_{\odot}$  and the distance between the lenses is taken uniformly in the range of  $d \in [0.1, 5] A.U.$ . The location of the lens from the observer is calculated from the probability function of microlensing detection  $d\Gamma/dx \propto \rho(x)\sqrt{x(1-x)}$  where  $x$  changes in the range of  $x \in [0, 1]$ . The velocity of the lens is taken by the combination of the global (Rahal et al. 2009) and the dispersion velocity (Binney & Tremaine 1987) of the disk and bulge. We take a thin disk for modeling the disk and take our line of sight towards the Galactic bulge with the latitude angle in the range of  $b \in [1, 2]$ .

For the source objects, the corresponding angles in the trajectory of the source system,  $\alpha$ ,  $\phi$  and  $\beta$  in Equation (7) is taken uniformly. The minimum impact parameter is in the range of  $u_0 \in$

$[0, 1]$ . we take the mass of the parent star from the Salpeter mass function in the range of  $M_{\star} \in [0.1, 3] M_{\odot}$ . Since the parent star is assumed to belong to the main sequence, the radius of the star is taken from equation (22). On the other hand the luminosity of the parent star can be obtained from (Eddington 1926):

$$L_{\star} = L_{\odot} \left( \frac{M_{\star}}{M_{\odot}} \right)^{3.5}. \quad (23)$$

For the parameters of the planet, the inclination angle  $\delta$  of the planetary plane to the line of sight is taken uniformly in the range of  $\delta \in [-\pi/2, \pi/2]$ . We take the mass of the planet in the range of  $M_p \in [0.1, 10] M_J$  and distance of the planet from the parent star in the range of  $a \in [0.01, 0.1] A.U.$  For the close-in Hot Jupiters at the distance less than  $\sim 0.05 A.U.$ , which are in our concern, the radius not only is a function of the planet's mass, it also depends on the distance of the planet from the parent star (Fortney et al. 2007). Close-in planets are heated by the parent star and their atmosphere inflates. For the hot planets, in contrast to the conventional relation between the mass and the size, the small mass planets, inflate more than the massive ones. We take the mass-radius-distance relation of Hot planets from Fortney et al. (2007).

Before performing Monte-Carlo simulation to count the number of events with the desired signal to the background flux, we do a first order estimation, just counting geometrically the number of planets that their trajectories cross the caustic lines. In our simulation we follow the path of the planet in the magnification pattern that has already been generated by the inverse-ray shooting and assign the magnification of the source object along its trajectory. We calculate the deviation of the flux along the path to identify any sharp peak in the light curve. This signature indicates a caustic crossing. Our simulation shows that in microlensing events with binary lens and for the condition of  $u_0 < 1$ , almost 36% of planets can cross the caustic lines. We obtain almost the same amount of the caustic crossing for the parent stars. We call this fraction of events with the caustic crossing as the geometrical criterion for the Hot Jupiter detection.

In reality we should measure the flux of source star and the enhancements due to the Hot Jupiter on the background light curve. First we assume a telescope with 1% photometric precision. We can change this criterion according to the size of telescope and a limiting magnitude on the brightness of the source star. With new techniques as defocusing of the telescope, we can achieve dispersions in the order of  $5 mmag$  with a medium size telescope where in terms of the relative flux dispersion to the background, it is in the order of  $10^{-4}$  (Southworth et al. 2009).

In our Monte-Carlo simulation we look to the maximum magnification of the planet when it crosses the caustic line and obtain the flux ratio of the planet to the source star at that point. Here we do not take into account the sampling rate of the observations of the event. A typical duration for the magnification of the planet during the caustic crossing is in the order of one hour and we assume to have a network of the telescopes to cover the event. For the photometric precision of 1%, in Table (1) we show the detection efficiency for various pass bands and atmospheric models of the Hot Jupiters. Longer wavelengths are more favorable for detection of the planet than the shorter ones. Also planets with high reradiating property (i.e.  $f = 2/3$  in this simulation), means less advection in the atmosphere are more favorable for the detection.

In order to see the sensitivity of the planet detection on the parameters of the model, we plot the detection efficiency in terms of the relevant parameters of the lens, source and planet in Figures (6) and (7) for three cases of photometric precision of  $10^{-2}$ ,  $10^{-3}$

Band :	<i>Optical</i>	<i>R</i>	<i>J</i>	<i>H</i>	<i>K</i>	<i>L</i>	<i>M</i>	<i>N</i>	<i>Q</i>	<i>Submillimeter</i>	Overall wave length
Wave length( <i>micrometer</i> )	0.55	0.825	1.25	1.65	2.2	3.45	4.7	10	20	450	
$A_B = 0 ; f = \frac{1}{3}$	0.01	0.04	0.13	0.23	0.36	0.67	0.94	2.62	5.33	10.74	0.01
$A_B = 0 ; f = \frac{2}{3}$	0.09	0.21	0.39	0.57	0.85	1.50	2.38	5.85	9.33	14.35	0.11
$A_B = 0.3 ; f = \frac{1}{3}$	0.03	0.06	0.13	0.21	0.32	0.57	0.80	2.06	4.45	9.81	0.03
$A_B = 0.3 ; f = \frac{2}{3}$	0.08	0.18	0.34	0.49	0.70	1.19	1.80	4.72	7.90	13.18	0.11
$A_B = 0.5 ; f = \frac{1}{3}$	0.05	0.07	0.13	0.20	0.29	0.51	0.70	1.60	3.66	9.0	0.06
$A_B = 0.5 ; f = \frac{2}{3}$	0.09	0.16	0.29	0.41	0.58	0.99	1.40	3.77	6.69	12.08	0.11

**Table 1.** Detection efficiency of Hot Jupiter for various optical, infrared and far-infrared bass-bands. The first column describes the atmospheric model of the planet, the second and the third columns represents the efficiency for the optical and red bands, the forth to the tenth columns shows the detection efficiency for the infra-red and far infrared pass bands. The eleventh column stands for the submillimeter and the last column shown the average detection efficiency over all the wavelengths, weighted to the spectrum of the planet.

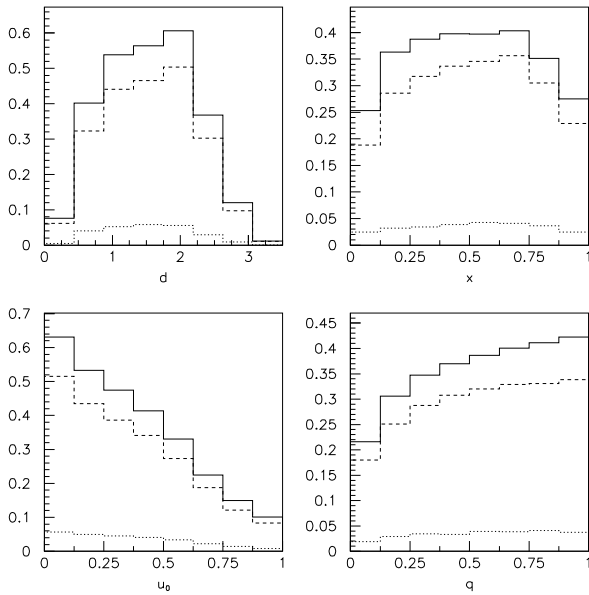


**Figure 6.** The detection efficiency for different parameters of lens for three different observational strategy with  $10^{-2}$  (dotted-line),  $10^{-3}$  (dashed-line) and  $10^{-4}$  (solid-line) photometric precision.

and  $10^{-4}$ . We ignore the irrelevant parameters that do not enter in the efficiency function. The detection efficiency function in terms of the lens and the source-planet parameters is given as follows:

(a) The distance between two lenses. Here the detection efficiency raises with increasing the distance between the two lenses and after a peak around  $\sim 2R_E$ , it decreases. The physical interpretation of this feature is due to the topological configuration of the caustic lines. It is shown in (Schneider & Weiss 1986) that for the case of  $q = 1$  and distance between the lenses in the range of  $[\frac{2}{\sqrt{8}}, 2]R_E$ , the caustic lines are topologically connected whereas beyond this range the caustic lines detach from each other. Having continues caustic lines increases the probability of caustic crossing both by the parent star and the planet.

(b) The second parameter is  $x = D_l/D_s$ , the relative distance of the lens to the source star. In the detection efficiency diagram,

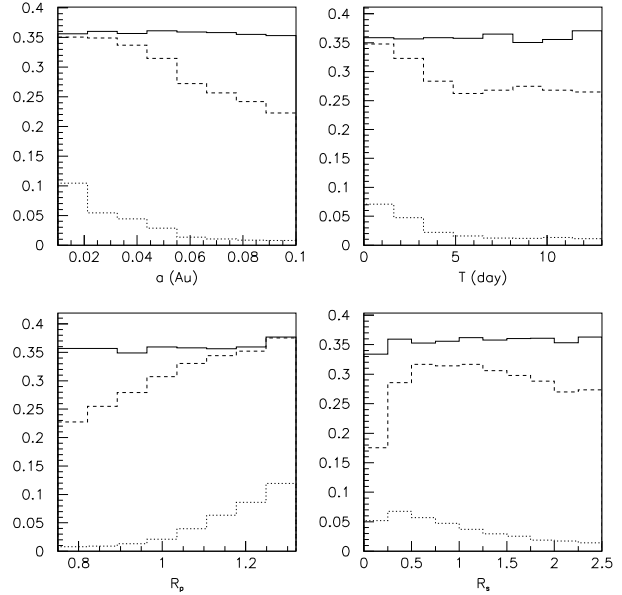


**Figure 7.** The detection efficiency for different parameters of the planet and the parent star for three different observational strategy with  $10^{-2}$  (dotted-line),  $10^{-3}$  (dashed-line) and  $10^{-4}$  (solid-line) photometric precision.

the efficiency reaches to the maximum value around  $\sim 0.5$  where the Einstein radius has the maximum size. A larger Einstein radius results in a longer duration for the microlensing event and a higher probability for the caustic crossing.

(c) The third parameter is the impact parameter. Decreasing the impact parameter increase the detection efficiency. Smaller impact parameter from the center of lens configuration increases the probability of the caustic crossing. On the other hand statistically the impact factor may also affect on the magnification of the light curve. We test this hypothesis amongst the simulated events showing that the small impact parameters results in a higher signal to the background flux.

(d) The ratio of the lens masses,  $q$ . It seems that changing  $q$  has a geometrical effect on the shape of the caustic lines, where

Photometric Precision :	$10^{-2}$	$10^{-3}$	$10^{-4}$
$\tau_p$	$1.34 \times 10^{-9}$	$1.34 \times 10^{-8}$	$1.57 \times 10^{-8}$
$N_p$	3	28	32

**Table 2.** The first line indicates the photometric precision, the second line is the corresponding optical depth of the hot Jupiter detection and the third line is the number of the planets that can be detected by monitoring  $10^7$  stars during 10 years towards the Galactic Bulge.

increasing it towards the symmetric shape,  $q = 1$  maximize the detection efficiency.

(e) The semi-major axis of the planet,  $a$ , shown in Figure (7). The Hot Jupiters reside in the range of  $[0.01, 0.1]Au$ . For the smaller  $a$  there is larger detection efficiency than the larger  $a$ . The dependence of the detection efficiency to the semi-major axis results from the reflection of the flux of the parent star from the planet, proportional to inverse square of the distance. The other effect is due to the intrinsic thermal luminosity of the planet, closer to the parent star makes the temperature of planet higher.

(d) Period of motion of planet,  $T$ . The dependence of the efficiency to the period is in the same way as the semi-major axis due to the Kepler's law. Shorter duration for the period of the planets resembles to the smaller semi-major axis.

(f) Radius of planet,  $R_p$ . The intrinsic flux of planet both in reflection of the parent star's light and thermal emission is proportional to square of radius of planet. Hence larger planets can be detected easier than the smaller ones.

(g) Radius of source star,  $R_s$ . The effect of the radius of the source star on the relative intensity of the planet to the parent star can be seen in equation (21). Increasing the radius of the star causes decreasing this ratio.

Finally we come to conclude on the possibility of detection of the hot Jupiters from this method. The comparison of the OGLE data with the model constructed from the Hipparcos data indicates that about  $f_p \sim 0.5 \times 10^{-2}$  fraction of the stars have hot Jupiters and very hot Jupiters (Gould et al.2006). On the other hand the radial velocity observations of the planets indicate that about  $f_p \sim 10^{-2}$  fraction of the solar type stars have hot Jupiters (Marcy et al. 2005). From the Monte-Carlo simulation we obtain the average detection efficiency  $\langle \epsilon_p \rangle$ , for the planet detection with three photometric precession of  $10^{-2}$ ,  $10^{-3}$  and  $10^{-4}$  as 0.03, 0.30 and 0.35. The optical depth for the planet detection can be obtained by

$$\tau_p = \langle \epsilon_p \rangle \times f_p \times \tau, \quad (24)$$

where  $\tau$  is the optical depth for the microlensing events towards a given direction. For the direction of the Galactic Bulge  $\tau = 4.48 \times 10^{-6}$  (Sumi et al. 2006), hence the optical depth for the planet detection is about  $\tau_p \simeq 10^{-8}$ . We can obtain the number of events for  $N_{bg}$  background stars with  $T$  exposure time as

$$N_p = \frac{\pi}{2} \frac{TN_{bg}}{\langle t_E \rangle} \times \tau_p, \quad (25)$$

where the average Einstein crossing time for the Galactic Bulge events is about  $\langle t_E \rangle = 28$  days. In Table (2) we provide the numerical values for the optical depth and number of events for each photometric cases.

## 5 CONCLUSION

In this work we examined the possibility of hot Jupiter detection through caustic crossing of a binary lens by a planet as the source object. The effect of this caustic crossing due to the small size of the planet is like an illumination on the microlensing light curve of the parent star. Taking the flux of the parent star as the background light and the illumination of the planet as the signal, we studied the physical characteristics of the planet as the orbital size, the atmospheric property and the size of the planet from one hand and the characteristics of the parent star and lens from the other hand on the observability of planet.

In the next step, we did a Monte-Carlo simulation to obtain the detection efficiency of the planet with this method. We showed that taking just geometrical caustic crossing of the planets, 36% of population can be illuminated. However in reality due to the photometric error the peak generated by the planet may not be detected. We used three different photometric precision in the observation and obtained the detection efficiency, assuming that we use a network of the telescopes to have enough sampling of data much less than one hour, a typical time of the caustic crossing of the planet. We showed that for longer pass-bands the detection efficiency is increased due to the more relative emissivity of planet compare to the parent star.

Finally we estimate the number of the Hot Jupiters that can be observed with this method towards the Galactic bulge. With a ten years monitoring of  $10^7$  stars towards the Galactic Bulge, we can detect in the order of 10 Hot Jupiter with this method. This observation may be done by the next generation of the microlensing surveys towards the Galactic Bulge.

## REFERENCES

- Barnes, J., Hut, P., 1986, Nature 324, L446.
- Beaulieu, J.-P., et al. 2006, Nature, 439, L437.
- Binney, S., & Tremaine, S. 1987, Galactic Dynamics (Princeton, NJ: Princeton Univ. Press), 78.
- Deming, D., & Seager, S., 2009 Nature, 462, L302.
- Eddington, A., 1926, The internal constitution of the stars (Cambridge Univ. Press).
- Fortney, J., et. al. ApJ 659, L1661.
- Gould, A., et al. 2010, preprint (arXiv:1001.0572)
- Gould, A., et al. 2006, Acta astron, 56, L1
- Graff, D. S., & Gaudi, B. S. 2000, ApJ, 538, L133.
- Greist, K., & Hu, W. 1992, ApJ 397, L362.
- Han, C., & Gould, A. 1996, ApJ 480, L196.
- Harrington, J. et al. 2006, Science 314, L623.
- Ida, S. & Lin, D. N. C., 2005, ApJ, 616, 567
- Kayser, R. & Refsdal, S. & Stabell, R. 1986, A&A 166, L36.
- Knutson, H. A., et al. 2007, Nature 447, L183.
- Lopez-Morales, M., & Seager, S., 2007, ApJ 667, 191.
- Mao, S., & Paczynski, B. 1991, ApJ, 374, L37.

## 8 *Sedighe Sajadian and Sohrab Rahvar*

- Marcy, G., Butler, R. P., Fischer, D., Vogt, S., Wright, J. T., Tinney, C. G., & Jones, H. R. A. 2005, *Prog. Theor. Phys. Suppl.*, 158, 24
- Milsztajn, A., & Lasserre, T., 2001, *Nucl. Phys. B(Proc. Suppl)*, 91, L413.
- Paczyński B., 1986, *ApJ* 304, L1.
- Pepper, J., et al. 2003 *Acta Astron.*, 53, L213.
- Rahal, Y. R., et al. 2009, *A&A*, 500, L1027.
- Rahvar, S. & Dominik, M., 2009, *MNRAS* 392, L1193.
- Rowe, J., et al. 2008, *ApJ* 689, L1345.
- Salpeter, E. E., 1995, *ApJ*, 121, L161.
- Schneider, P. & Wiess, A., 1986, *A&A* 164, L237.
- Schneider, P. & Wiess, A., 1987, *A&A* 171, L49.
- Southworth, J. et al. 2009, *MNRAS*, 396, 1023
- Sumi, T., et al. 2006, *ApJ* 636, 240.
- Wambsganss, J., 1999, *J. Comput. Appl. Math.*, 109, L353.